PHOTONIC SENSORS / Vol. 6, No. 4, 2016: 333–338

Spectra Power and Bandwidth of Fiber Bragg Grating Under Influence of Gradient Strain

Qinpeng LIU*, Xueguang QIAO, Zhen'an JIA, and Haiwei FU

Key Laboratory on Photoelectric Oil-Gas Logging and Detecting (Ministry of Education), Xi'an Shiyou University, Xi'an, 710065, China

*Corresponding author: Qinpeng LIU E-mail: lqp1977@163.com

Abstract: The reflective spectrum power and the bandwidth of the fiber Bragg grating (FBG) under gradient strain are researched and experimentally demonstrated. The gradient strain is applied on the FBG, which can induce FBG bandwidth broadening, resulting in the variation of reflective power. Based on the coupled-mode theory and transfer matrix method, the segmental linear relationship between the gradient strain, the reflective power, and the bandwidth is simulated and analyzed, and the influence of the FBG length on the reflective spectrum is analyzed. In the experiment, the strict gradient stain device is designed; the experimental results indicate that the reflective optic power and the bandwidth of the FBG under gradient stain are concerned with the length of the FBG. Experimental results are well consistent with the theoretical analysis, which have important guiding significance in the FBG dynamic sensing.

Keywords: Fiber Bragg grating; gradient strain; reflective spectrum power; reflective spectrum bandwidth

Citation: Qinpeng LIU, Xueguang QIAO, Zhen'an JIA, and Haiwei FU, "Spectra Power and Bandwidth of Fiber Bragg Grating Under Influence of Gradient Strain," *Photonic Sensors*, 2016, 6(4): 333–338.

1. Introduction

As an important wavelength sensitive device, a fiber Bragg grating (FBG) has been widely studied and applied [1–5]. Most of the researches focus on the wavelength sensing technology and theory, but when the inhomogeneous field applying on the FBG, such as the gradient stain and gradient temperature, acts on the grating range of the FBG, which can lead to the FBG chirping, and the reflective spectrum shows new features, such as reflective power and reflective bandwidth [6–10]. It has many methods to form inhomogeneous refractive-index modulation, such as designing the grating structure [11, 12], introducing a strain gradient by designing an especial fabrication structure [13, 14], and etching the FBG [15]. The essence of the inhomogeneous field modulation induces a refractive-index gradient. The spatially varying structure of the fiber grating can be divided into several sections called the effective-interaction sub-regions, each effective-interaction sub-region possesses an independent sensing ability, whose relationship to the gradient distribution of environmental parameters has been researched [16], and the reflective spectrum of the linear chirp FBG is analyzed by using a four-order Runge-Kutta method and transfer matrix method [17]. The results show that the linearly chirped fiber Bragg gratings can broaden the bandwidth. But all of the researches at present do not provide more

Received: 22 April 2016 / Revised: 18 August 2016
© The Author(s) 2016. This article is published with open access at Springerlink.com
DOI: 10.1007/s13320-016-0325-9
Article type: Regular

complete discussion of reflective spectrum power and the bandwidth for the whole range, which is not the accurate response relationship between the bandwidth broadening and the reflective optic spectra power (ROSP), and the relationship between them is necessary to further research, which is a precondition to the FBG wavelength and intensity sensing.

In this paper, the reflective optic spectra power (ROSP) and the bandwidth of the FBG are elaborately researched based on the coupled-mode theory and transfer matrix method (TMM). The bandwidth and the spectra power of the FBG under the gradient strain are theoretically analyzed, and the relationship between the bandwidth and coefficient of chirping is demonstrated. The significant relationship between the ROSP and chirping coefficient is also theoretically simulated, and the relationship between them is fully proposed. In numerous methods, the external modulating method by designing an especial transducer is simple and easy to realize. At the most basic physical quantities, the gradient stain has typically representative meaning. So the gradient-strain device is accordingly designed; the experimental results show a good agreement with the theoretical analysis, which is an important basis for designing an intensity modulation sensor for the dynamic and static measurement.

2. Theory and analysis

According to the coupled-mode theory, the forward (reference) modes and backward propagation modes (signals) satisfy the following equations:

$$\begin{cases} \dfrac{dR}{dz} = \mathrm{i}\left(\delta + \sigma - \dfrac{1}{2}\dfrac{d\phi(z)}{dz}\right)R(z) + \mathrm{i}kS(z) \\ \dfrac{dS}{dz} = -\mathrm{i}\left(\delta + \sigma - \dfrac{1}{2}\dfrac{d\phi(z)}{dz}\right)S(z) - \mathrm{i}k^{*}R(z) \end{cases} \tag{1}$$

where $\delta = 2\pi n_{\mathrm{eff}}(1/\lambda - 1/\lambda_B)$, $\sigma = 2\pi\Delta n/\lambda$, and $d\varphi(z)/dz = 2\pi n_{\mathrm{eff}} zC/\lambda_B^2$ are the dc-components of self-coupling coefficient, respectively. k is an alternating current coupling coefficient. λ_B is the Bragg wavelength, and C is the chirping coefficient of the fiber grating, which is defined as $d\lambda_{\mathrm{B}}/dz$. According to (1), the reflective optic spectra of the fiber grating is given as

$$R(\lambda) = \frac{\sinh^2(\sqrt{k^2-\sigma^2}L)}{\cosh^2(\sqrt{k^2-\sigma^2}L) - \sigma^2/k^2}. \tag{2}$$

Assuming the gradient strain is applied to the FBG, the period $\Lambda(z)$ of the fiber Grating is defined as

$$\Lambda(z) = \Lambda_0[1 - gz] \qquad -\frac{L}{2} \le z \le \frac{L}{2} \tag{3}$$

where Λ_0 is the initial period, L is the length of the fiber grating, and g is the strain gradient, which is defined as $g = d\varepsilon(z)/dz$. Based on the above theoretical model, the FBG can be divided into several sections called the effective-interaction sub-regions, and each sub-region possesses an independent sensing ability, so TMM is the best choose to analyze the reflective optic spectra. Combined with the boundary conditions and transfer matrix, we can further research the relationship between the reflective optic spectra power and chirping coefficient. Because the reflective optic spectrum of the FBG is narrow, the spectrum power density of the sensing source should be used as constant, and the ROSP change ΔP of the chirping FBG can be expressed as

$$\Delta P = \int_{\lambda_1}^{\lambda_2} \eta P_{\mathrm{BBs}} R(\lambda) d\lambda \tag{4}$$

where λ_1 and λ_2 is the minimum resonance wavelength and maximum resonance wavelength, respectively. η is the insertion of loss, and P_{BBS} is the spectrum power density of the sensing source. Then the bandwidth and ROSP of the linear chirping FBG can be simulated by using the TMM. Base on the previous analysis, assume the strain gradient is same, that is to say, the coefficient of chirping is same, and the reflective power variation of the FBG should depend on the length of the FBG, because the ROSP is the result within the scope of the integral.

Therefore, the influence of the length should be considered. For comparison, the ROSP is given in the normalized power. Figure 1 presents the changing rule of the 10-dB bandwidth with 10 mm, 20 mm, and 40 mm long FBGs. The simulated results demonstrate that the bandwidth increases with the chirping coefficient for different length FBGs. The longer FBG means the higher sensitivity and the better linearity. Meanwhile, the relationship between the bandwidth and the chirping coefficient is not strictly linear in the whole range, while it is piecewise linear function, and the shorter FBG means more seriously nonlinear. In addition, the focus of this paper is the relationship between the ROSP and the chirped coefficient, because compared with bandwidth sensing, it is more suitable for the dynamic test. To facilitate the analysis, the reflective optic spectra normalized power (ROSPN) is utilized, and based on the previous theory, the ROSPN can be obtained for different FBGs, as shown in Fig. 2, in which the insert shows the reflective optic spectra of 10 mm, 20 mm, and 40 mm long FBGs, respectively. It can be seen that the ROSPN increases as the chirping coefficient increases. The longer the FBG is, the more sensitivity to the ROSPN it is. The ROSPN is inclined to be saturated with an increase in the chirping coefficient. This phenomenon is due to that the partial sub-region loses the independent sensing ability when the large strain gradient is applied on the FBG. When the chirping coefficient is small, the FBG has been divided into several effective-interaction sub-regions; it can be generated with the linear bandwidth and power in the chirping coefficient. The relationship is extremely important for intensity sensing, which also determines the linear range of the sensor.

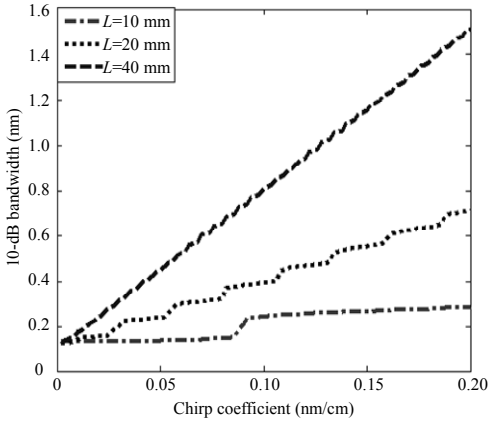

Fig. 1 Relationship between the 10-dB bandwidth and chirping coefficient.

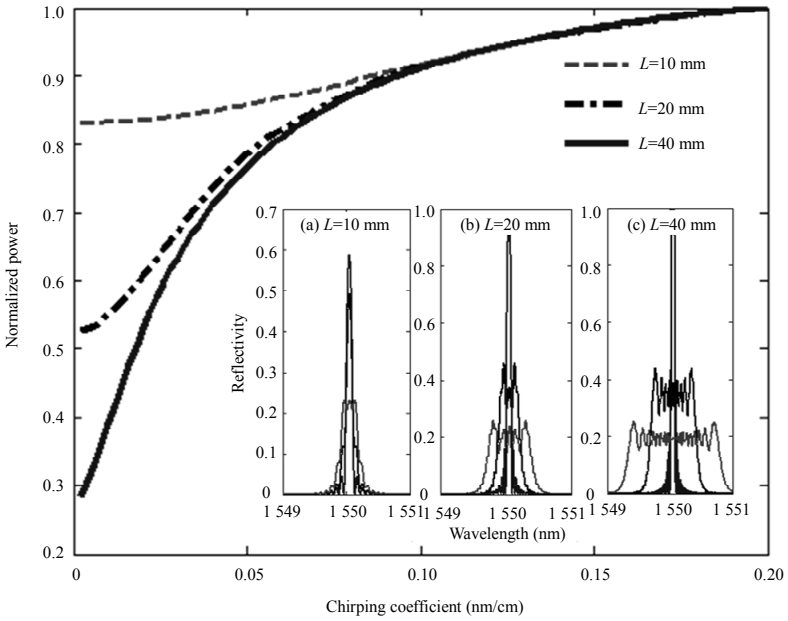

Fig. 2 Relationship between the normalized power and chirping coefficient.

3. Experiments

To demonstrate the relationship between the ROSPN and chirping coefficient, the FBGs used in the experiment are 10 mm, 20 mm, and 45 mm long with the 3-dB bandwidth of 0.28 nm, 0.214 nm, and 0.195 nm. Light from the broad-band source (BBS) is coupled into the FBG via a 3-dB coupler, and the power and the bandwidth of the reflective spectrum are monitored by the optical spectrum analyzer (MS9740A) with the resolution of 0.02 nm. The linear strain is elaborately provided by an especial cantilever. The setup is shown in Fig. 3. The structure of the especial cantilever is designed, and their strain distribution under the influence of pressure is shown in Fig. 4. It can be seen that the strain distributions are gradient in the FBG range, the strain gradient is determined, and the chirping coefficient of the fiber grating is also is accordingly determined. A linear strain distribution is a precondition for the broadening around the central wavelength, FBGs have been fabricated on the upper surface of the cantilever, the geometric center of FBGs is located in the middle position of the cantilever, and the chirping coefficient is modulated by applying side pressure.

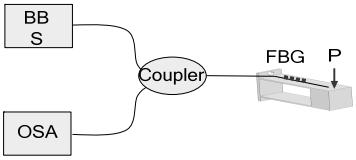

Fig. 3 Schematic diagram of the experimental setup.

The response of the ROSP is measured under the side-applied pressure, as shown in Fig. 5. It can be seen that the ROSP increases with an increase in the stain gradient. As the ROSP increases, the ROSP becomes saturated, that is to say, with an increase in the chirping coefficient (strain gradient), the rate of change reduces, and in the meantime, if the grating is longer, its power change become more sensitive to the strain gradient. The change in the ROSP is not strictly linearly varied with the side-applied pressure in the whole range, but it is piecewise linear functions. The 10-dB bandwidth of the grating is measured under the side-applied pressure, as depicted in Fig. 6. The broadening of the spectra bandwidth varies with applying side pressure. The change in the bandwidth is also not strictly linearly varied with pressure, and FBGs with different lengths have different linear responses. It is obvious that the FBG with the length of 45 mm has the best linear response in the experiment, which has higher bandwidth sensitivity. The longer FBG is, the more sensitive and linear its bandwidth broadening becomes. On the contrary, the shorter the length is, the worse the linearity is, and the lower the sensitivity is. The relationship is extremely important for the intensity sensing, and the linear range dominates the sensing range. Meanwhile, based on the above analysis, the shorter the grating is, the less chirping it will be. It also has great significances to FBG wavelength sensing.

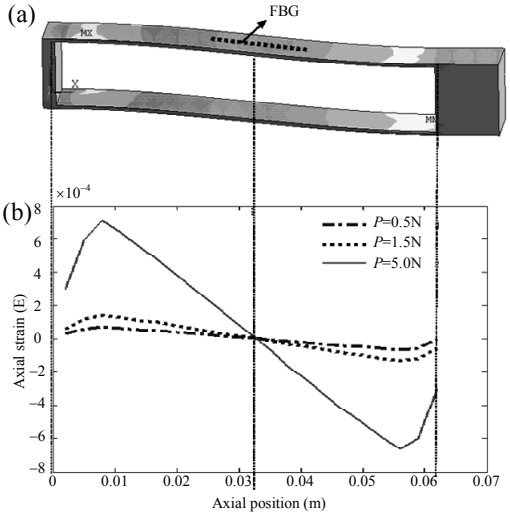

Fig. 4 Surface-strain distribution of the especial cantilever.

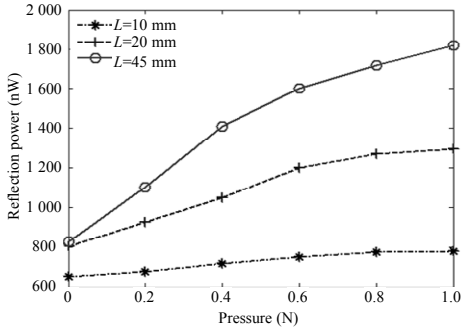

Fig. 5 Relationship between the reflective power and pressure.

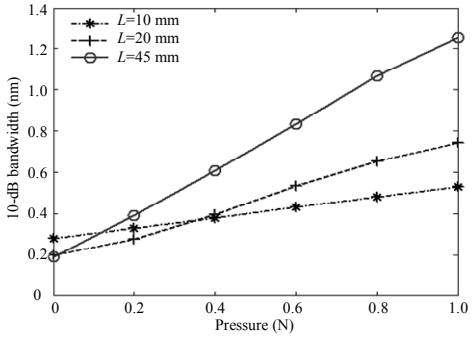

Fig. 6 Relationship between the 10-dB bandwidth and pressure.

4. Conclusions

In this paper, the ROSPN and bandwidth of the FBG under the influence of the linear strain have been theoretically simulated and experimentally demonstrated. The theoretical analysis shows the relationship among the ROSPN, the chirping coefficient, and bandwidth. The main conclusions are as follows:

(1) The relationship among the ROSPN, the chirping coefficient, and bandwidth are not strictly linear in the whole range, and it is piecewise linear functions.

(2) The shorter the grating is, the more insensitivity to the linear strain its bandwidth broadening is. The longer the grating is, the more sensitive its bandwidth broadening becomes under the same condition, and the better the linearity is.

(3) The shorter the grating is, the more insensitivity to linear strain its ROSPN is. The longer the grating is, the more sensitive it becomes under the same condition, and the worse the linearity is. The collusions are very important for FBG intensity sensing, which have guiding significance for the structure design and dynamic range of the FBG intensity sensing. In addition, the analysis indicates that it will have the shorter grating and less chirping. It has also great significances to FBG wavelength sensing in the miniaturization of device.

Acknowledgment

This work was supported in part by the National Natural Science Foundation of China (No. 61077006, 60727004, and 61077060), in part by the Ministry of Education Project of Science and Technology Innovation (No. Z08119), and in part by the Shannxi Province National Science Foundation under Grant 2016JM6055.

Open Access This article is distributed under the terms of the Creative Commons Attribution 4.0 International License (http://creativecommons.org/ licenses/by/4.0/), which permits unrestricted use, distribution, and reproduction in any medium, provided you give appropriate credit to the original author(s) and the source, provide a link to the Creative Commons license, and indicate if changes were made.

References

[1] T. Li, Y. Tan, Z. Zhou, L. Cai, S. Liu, Z. He, *et al.*, "Study on the non-contact FBG vibration sensor and its application," *Photonic Sensors*, 2015, 5(2): 128–136.

[2] L. Li, D. Zhang, H. Liu, Y. Guo, and F. Zhu, "Design of an enhanced sensitivity FBG strain sensor and application in highway bridge engineering," *Photonic Sensors*, 2014, 4(2): 162–167.

[3] J. Wang, T. Liu, G. Song, H. Xie, L. Li, X. Deng, *et al.*, "Fiber Bragg grating (FBG) sensors used in coal mines," *Photonic Sensors*, 2014, 4(2): 120–124.

[4] S. Li and M. Zhou, "Long-term mechanical properties of smart cable based on FBG desensitized encapsulation sensors," *Photonic Sensors*, 2014, 4(3): 236–241.

[5] X. Zhu, "Aluminum alloy material structure impact localization by using FBG sensors," *Photonic Sensors*, 2014, 4(4): 344–348.

[6] Y. G. Han, X. Y. Dong, J. H. Lee, and S. B. Lee, "Simultaneous measurement of bending and temperature based on a single sampled chirped fiber Bragg grating embedded on a flexible cantilever beam," *Optics Letter*, 2006, 31(19): 2839–2841.

[7] T. Guo, B. Liu, and X. Y. Dong, "Linear and Gaussian chirped fiber Bragg grating and its applications in fiber-optic filtering and sensing systems," *IEEE Photonics Technology Letters*, 2007, 19(14): 663–665.

[8] B. Q. Jiang, J. L. Zhao, C. Qin, and F. Fan, "A bandwidth-tuning device based on polymer-packaged fiber Bragg grating," *IEEE Photonics Technology Letters*, 2011, 23(17): 1225–1227.

[9] X. G. Qiao, Y. P. Wang, H. Z. Yang, G. Tuan, Q. Z. Rong, L. Ling, *et al.*, "Ultrahigh-temperature chirped fiber Bragg grating through thermal activation," *IEEE Photonics Technology Letters*, 2015, 27(12): 1305–1308.

[10] M. Abtahi, A. D. Simard, S. Doucet, L. Sophie, and L. A. Rusch, "Characterization of a linearly chirped FBG under local temperature variations for spectral shaping applications," *Journal of Lightwave Technology*, 2011, 23(5): 750–755.

[11] J. L. Cruz, L. Dong, S. Barcelos, and L. Reekie, "Fiber Bragg gratings with various chirp profiles made in etched tapers," *Applied Optics*, 1996, 35(34): 6781–6787.

[12] L. Dong, J. L. Cruz, L. Reekie, and J. A. Tocknott, "Chirped fiber Bragg gratings fabricated using etched tapers," *Optical Fiber Technology*, 1995, 1(4): 363–368.

[13] Y. N. Zhu, P. Shu. C. Lu, M. B. Lacquet, P. L. Swart, A. A. Chtcherbakov, *et al*., "Temperature insensitive measurements of static displacements using a fiber Bragg grating," *Optics Express*, 2003, 11(16): 1918–1924.

[14] B. Yin, Y. L. Bai, and Y. H. Qi, "Study on tapered chirped fiber grating filter," *Acta Physica Sinica*, 2013, 62(21): 214213–214213.

[15] H. Z. Yang, K. S. Lim, X. G. Qiao, W. Y. Chong, Y. K. Cheong, W. H. Lim, *et al*., "Reflection spectra of etched FBGs under the influence of axial contraction and stress-induced index change," *Optics Express*, 2013, 21(12): 14808–14815.

[16] G. Tuan , B, Liu, W. G. Zhang, G. Y. Kai, Q. D. Zhao, and X. Y. Dong, "Research on optical fiber grating chirp-sensing technology," *Acta Physica Sinica*, 2008, 28(5): 828–834.

[17] J. J. Wei, Y. P. Liang, and T. L. Dai. "Numerical analysis of reflection spectrum of linearly chirped fiber Bragg gratings," *Laser Technology*, 2012, 36(5): 607–611.